Simple, Fast and Accurate Maximum Power Point Tracking Converter for Thermoelectric Generators

Andrea Montecucco, Jonathan Siviter and Andrew R. Knox
School of Engineering
University of Glasgow
Glasgow, United Kingdom
andrew.knox@glasgow.ac.uk

Abstract—**Thermoelectric generators (TEGs) can harvest thermal energy producing electrical power from a temperature gradient. They are often employed in dynamic thermal environments, therefore it is important to quickly and precisely track the best operating point to maximize the power production.**

This paper presents an innovative way to measure the open-circuit TEG voltage without disconnecting the load, to be used in a Maximum Power Point Tracking (MPPT) algorithm based on the open-circuit voltage method. The proposed system is composed of a buck converter with embedded microcontroller, which is used both to compute the MPPT algorithm and to control the charging of a lead-acid battery. The prototype converter is tested using a TEG system and it can accurately set the optimum operating point almost instantaneously and without significant computational power requirements.

I. INTRODUCTION

A thermoelectric generator (TEG) is a solid-state device that can convert thermal energy from a temperature gradient into electrical energy. It can use almost any source of thermal energy and it has a number of advantages over other energy conversion methods: it is compact, light in weight, reliable, and has no mechanical moving parts, thus it has no vibration or maintenance requirement and it is silent in operation.

Due to cost and low efficiency -around 4%- the use of TEGs has been in the past restricted to specialized medical, military, remote and space applications. However in recent years an increasing public awareness of environmental issues has resulted in research into alternative commercial methods of generating electrical power and thermoelectrics has emerged as a sustainable source of electricity [1]. Moreover the efficiency of TEGs is improving and the device cost is decreasing. Consequently, TEGs can now be successfully employed to harvest the heat energy rejected by other processes (automotive [2], [3], stove [4], [5], or power stations [6], [7]) or to increase the system efficiency in symbiotic applications [8], [9]. 'Mass-produced' energy scavenging applications such as exhaust gas systems are likely to lead to a further reduction of TE devices' cost. In applications of waste heat harvesting the input power is essentially free; therefore the low conversion efficiency is not a serious drawback, while it is important to maximize the power produced.

TEGs can be modeled as a voltage source in series with an internal resistance [10]. This behavior can be clearly identified from undertaking an electrical characterization, as it will be shown later. When placed between a hot and a cold side, they produce an open-circuit voltage

$$V_{OC} = \alpha\Delta T \quad (1)$$

where α is the Seebeck coefficient (characteristic of the materials used) and ΔT is the temperature gradient across the TEG. The internal resistance is a function of the average temperature of the module, while the Seebeck coefficient, and the output current and voltage depend on the temperature gradient [11]. If R_{int} is the internal resistance and R_{load} is a resistive load connected to the TEG, the current flowing in the circuit is

$$I = \frac{\alpha\Delta T}{R_{int}+R_{load}} \quad (2)$$

For the theorem of maximum power transfer, when the load matches the internal resistance ($R_{load}=R_{int}=R$) the maximum output power is achieved and it is equal to

$$P_{max} = \frac{(\alpha\Delta T)^2}{4R}. \quad (3)$$

When this condition is verified the voltage on the load V_{load} is exactly half of V_{OC}.

Load matching is difficult to achieve during transients and in an environment where temperatures vary dynamically, e.g. in an exhaust gas system. Therefore it is necessary to use power electronics controlled by a Maximum Power Point Tracking (MPPT) algorithm to interface the load to the TEGs

European Thermodynamics Ltd. and the Robin Kerr Watson Trust

978-1-4673-0803-8/12/$31.00 ©2012 IEEE

in such a way to match the virtual load seen by the TEGs to their actual internal resistance. Thus a DC-DC converter is connected between the TEGs and the load; by changing the duty cycle of the converter it is possible modify the virtual load seen by the TEGs. In literature, the most used MPPT algorithms for TEGs are the Perturb & Observe (P&O) [5], [12], [13] and the Incremental Impedance (INC) [14], [15]. However most of these algorithms had been originally developed for photovoltaic (PV) systems, whose electrical characteristic is logarithmic; on the contrary the electrical characteristic of TEGs is linear, therefore an easier way to maximize the power produced by the TEGs would be setting the voltage on the load to be half of V_{OC}. Such a MPPT algorithm measures V_{OC} and then sets the input voltage of the DC-DC converter to half this value, controlling the duty cycle δ of the converter, e.g. $\delta=V_{OUT}/V_{IN}$ for a Buck converter. This MPPT method is simpler and requires less computational power than the P&O and INC methods, but it works only for thermoelectric generators. However, while measuring the open-circuit voltage the DC-DC converter would need to be disconnected from the TEGs, thus periodically no power flows to the load [14] and the converter undergoes frequent transients. Nagayoshi *et al.* [16] measure the open-circuit voltage with the converter disconnected, then start the feedback control and assume that the internal resistance of the TEGs remains constant; however the Maximum Power Point (MPP) varies considerably depending on the operating conditions, as it will be shown in Section III, therefore this solution is not very efficient in a practical application.

This paper presents an innovative way to measure the open-circuit TEG voltage V_{OC} without the need of disconnecting the TEGs from the converter. In this way the converter does not need to undergo a transient each time the TEGs are disconnected and the harvested power is always maximized. An accurate measure of V_{OC} is enough to set the optimum operating point, exploiting the linearity of the electrical characteristic of the TEGs, so that this system does not require much control design and code complexity, while achieving even better performance if compared to the aforementioned techniques. We believe that such a system can improve the capture of power produced by the TEGs in steady-state and dynamic thermal environments, thus improving the system efficiency and helping thermoelectric systems to be more employed and better exploited in industrial applications.

II. TEG POWER CONVERSION SYSTEM

The proposed system aims at maximizing the electrical power produced by thermoelectric generators, effectively charging a lead-acid battery load. As explained in the Introduction, the proposed MPPT converter uses the open-circuit method to set the operating point to $V_{OC}/2$. The innovation presented lies in how the measure of V_{OC} is achieved: periodically (depending on the desired response speed) the input capacitors are disconnected for a few switching cycles and the microcontroller is timed to measure the TEGs' voltage while the converter's switch is off (t_{off}). This technique is described in sub-section C, while experimental results and considerations can be found in sections III and IV.

Fig. 1 depicts the diagram of the whole system. The TEGs are represented by a voltage source in series with their internal resistance and they are connected to a DC-DC Buck converter with the battery as load. An inexpensive microcontroller controls both the high-frequency switching of the converter and a low-side switch connected to the input capacitors. The microcontroller is programmed with the MPPT algorithm and with the battery charging routine.

The thermoelectric generators and the test rig used to test the MPPT converter are described in the sub-section A. The DC-DC converter is treated in the sub-section B, while the control of the battery charging and the MPPT algorithm are explained in the sub-sections C and D respectively.

A. Thermoelectric Generators and Test Rig

The test rig used to test TEGs is composed of a "hot" side and a "cold" side. The former is a copper block which contains two high-temperature high-power silicon-nitride heaters. Each heater is rated to a maximum of 500Wwith a surface temperature of 1250°C and it is powered by an AC power supply. The "cold" side is constructed from a second copper block through which water is pumped from a chiller unit. The heater block is able to provide 1kW of thermal power at a temperature in excess of 700°C. The chiller unit can remove up to 1kW from the working fluid and it can maintain the working fluid at an adjustable temperature between 5°C and 25°C ±0.1°C. Up to four 5x5cm TEGs can be sandwiched between the hot temperature and cold temperature blocks, and their output leads can be connected to an electronic load or to any other desired load. Thermocouple sensors are fitted touching the TEGs' hot and cold faces in order to obtain precise temperature measurements, which are read by a data logger with internal reference temperature. All the instruments used are controlled by a computer using the software VEE Pro by Agilent; the program used does a precise electrical characterisation of the modules at different temperature gradients, setting different loads in sequence, always at the same temperature difference.

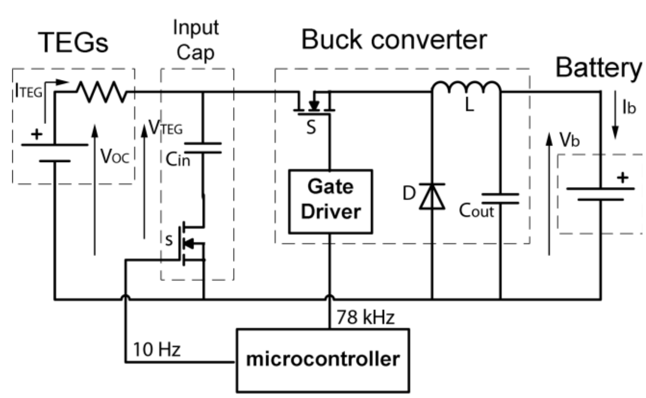

Figure 1. Diagram of the whole system used in the experiment.

For all the experiments presented in this paper four TEG modules from European Thermodynamics Ltd (product code GM250-127-14-16) have been used and characterised, when electrically connected in series. In Fig. 2 are shown the Voltage vs Current (V-I) and the Power vs Current (P-I) characteristics for two different temperature gradients (175°C and 220°C). This figure contains both the experimental values and a mathematical fitting to show the remaining points, among which the open-circuit voltage is very important. As can be observed, for every temperature gradient the V-I characteristic is a straight line, which proves that TEGs can be modeled in steady-state as a voltage source (of value V_{OC}) in series with a resistor (of value R_{int}). As a consequence, the maximum power point is confirmed to be at half of the open-circuit voltage. Moreover it is interesting to note that the slope of the two V-I lines is not the same, which indicates a change in the internal resistance of the TEGs in accordance with the temperature gradient across the device.

B. DC-DC Converter

A Buck converter has been chosen in order to interface the max input (TEG) voltage of 35V to the 12V of the battery. It has been designed to provide an output nominal power of 70W at 14.4V output. The circuit parameters are as follows: L=150μH, C_{in}=147μF, C_{out}=200μF. The switching frequency is 78kHz.

The input capacitors can be switched on and off the circuit by a low-side n-MOSFET controlled by the microcontroller; it also sends the Pulse Width Modulation (PWM) signal to the opto-isolated gate driver which controls the on/off state of the high-side n-MOSFET of the converter. The whole control operation is left to the microcontroller (PIC16F690), which performs two main tasks, as it is programmed to maximise the power generated by the TEGs and to manage the charging of the lead-acid battery. Both tasks are described in the two following sub-sections.

C. MPPT Algorithm

The dynamic electrical response of TEGs is in the range of nanoseconds [12] and this is the characteristic exploited by the proposed open-circuit measurement technique.

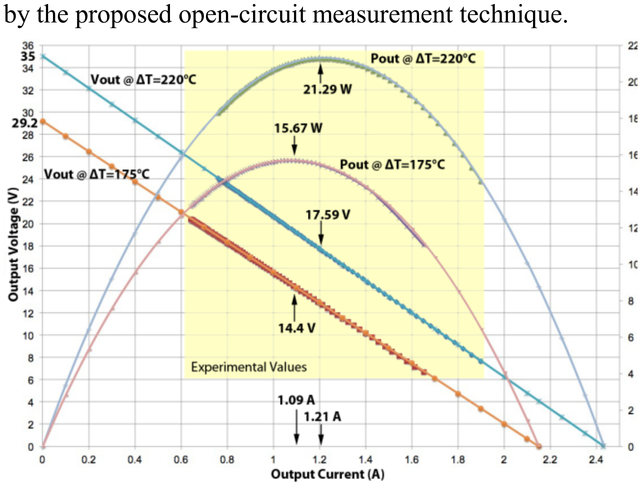

Figure 2. V-I and P-I characteristics for two temperature gradients (175°C and 220°C) of the four TEGs used electrically connected in series.

First, consider a DC-DC Buck converter without any input capacitor; the Buck has got a switch in series with the TEGs hence for the time that the Pulse Width Modulation (PWM) is at low state the TEGs' voltage goes instantaneously to V_{OC}. The electrical transient response of the TEGs is much faster than the switching frequency of the converter, set at 78kHz, therefore it does not affect the operation of the converter. If the microcontroller is timed to measure the TEGs' voltage when this happens, then the duty cycle that needs to be set in order to work at MPP is

$$\delta = \frac{V_{out}}{V_{OC}/_2} = \frac{V_{out}}{V_{MPP}} \tag{4}$$

where V_{out} can be considered fixed and constant during the switching period, because it is set by the battery. However, when the input capacitors are not connected, there is no harvesting of power from the TEGs, because the TEGs are not able to supply a high spike of current during t_{on} of the PWM, as they have a fairly high internal resistance. At the same time it would not be necessary to measure V_{OC} at every switching cycle because the thermal transients in TEG applications are several orders of magnitude longer than the switching period of the converter and the battery can deal with any sudden load change. Therefore it has been chosen to disconnect the input capacitors every 100ms, giving the MPPT algorithm a response frequency of 10Hz.

A low-side n-MOSFET has been connected to the input capacitors and is controlled by the microcontroller: every 100ms the input capacitors are disconnected and a new value for V_{MPP} is calculated, while the Buck converter is still connected to the load and to the TEGs. The only drawback with this approach is that the average output current is less than I_{MPP} during the few switching cycles needed by the microcontroller to perform the routine; this is not a significant loss, and it will be shown by experimental results in section III that this MPPT converter sets always and almost instantaneously the Maximum Power operating Point (MPP). In fact the MPP is confirmed to be at $V_{OC}/2$; this is always true even during a thermal transient, because the thermal time constant is much longer than the electrical response.

A great advantage of this MPPT scheme is that it is easily implemented. Unlike the P&O and INC methods, there is no need to measure currents, there is no requirement to design in the frequency domain and there are no issues with algorithm step size. Moreover, it is easily adaptable to changes in the converter parameters and it can be easily modified to control a Buck-Boost DC-DC converter.

D. Battery Management

The battery charging process used in the proposed system is similar to [17]. A 12V valve-regulated lead-acid battery has the characteristic shown in Fig. 3, in which the voltage is drawn against the State of Charge (SoC), for different charging rates; C is the battery capacity in [Ah] and for example C_4 corresponds to a charging current of $C/4$ Amps. 100% charge can be reached only with a small charge rate. If the battery voltage is less than 10.2V at 25°C, which means that the battery is deeply discharged or one or more cells are shorted [18], a trickle-charge I_{trckl} will first be used (pink-shaded area nearest the origin). Once the trickle-charge threshold is exceeded, the bulk-charging process with an initial maximum charging current $I_{max\_i}=C/4$ because battery manufacturers recommend charge rates in the *C/20* to *C/3* range [19] (light-blue area labeled MPPT). When the battery voltage rises above 14.4V the microcontroller decreases the maximum charging current I_{max} by a factor of 2; as soon as this happens the battery voltage falls between 12.8V and 14.4V. The state of charge increases until 14.4V is reached again and the same process is repeated until *C/64* is reached and the voltage is stable at 14.4V, which indicates a 100% SoC (over-charge, green area at the top right of the MPPT area). At this point I_{trckl} is set again to compensate the leakage current. The voltage limits are compensated depending on the battery temperature.

E. Microcontroller Flowchart

The microcontroller measures the TEG voltage at the converter input, the battery voltage at the converter output, and the ambient temperature using a thermistor IC, which is necessary to compensate the voltage limits of the battery with temperature changes. A Hall-effect current transducer is employed to measure the battery current, which is necessary to control the charging of the battery, but it would not be required to perform the MPPT function on its own. The microcontroller controls the gate driver connected to the high-side n-MOSFET of the Buck converter with a 78kHz, 8-bit on-chip PWM, and it directly drives the low-side n-MOSFET used to switch the input capacitors on and off the circuit at 10Hz frequency. For debug purposes only, the microcontroller also controls a four-line alphanumeric liquid-crystal display (LCD). The control algorithm is explained by the flowchart in Fig. 4.

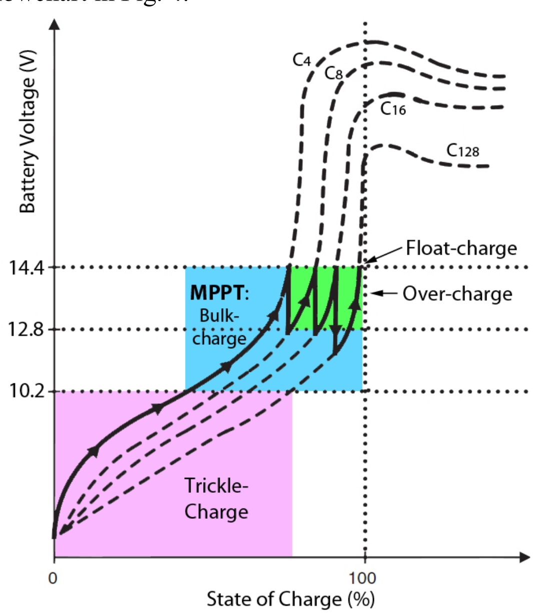

Figure 3. Voltage vs SoC of a lead-acid battery, for different charging rates (C_n=*C/n*). Charging process in bold arrow line.

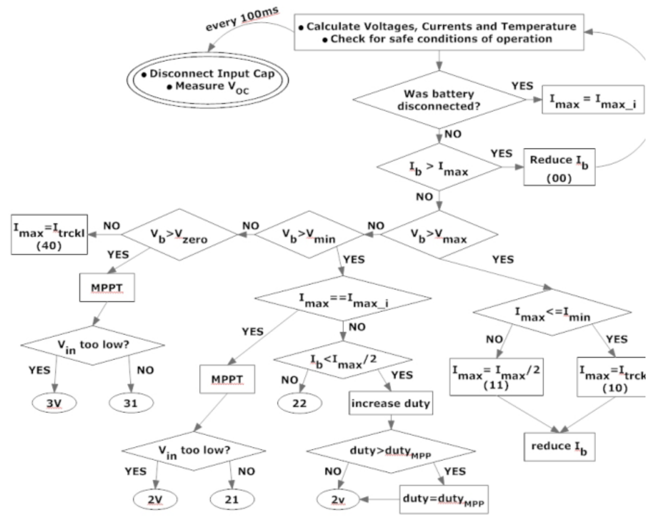

Figure 4. Flowchart of the code programmed to the microcontroller.

Every 100ms the capacitors are disconnected and the duty cycle needed to set the MPP, δ_{MPP}, is calculated and stored. If V_{TEG} is too close to V_b, the maximum allowable duty cycle is set (90%).The microcontroller sets such a value only if it is compatible with the actual SoC of the battery.

After checking if the battery was previously disconnected, the controller reduces the current if it is greater than I_{max}; this is done by decreasing the duty cycle by a factor proportional to the difference I_{max}-I_b. Otherwise the microcontroller will decide if to maximise the power or to set a new value for I_{max}:

1. V_b>14.4V: I_{max} is reduced down to I_{trckl}
2. 12.8V<V_b≤14.4V: if $I_{max}=I_{max\_i}$ MPPT; otherwise the duty cycle is not changed unless I_b< $I_{max}/2$, which indicates that the power produced is decreasing, therefore the duty cycle is increased by *0.39%*
3. 10.2V<V_b≤12.8V: MPPT
4. V_b<10.2V: $I_{max}=I_{trckl}$

In 2. the duty cycle is increased only if the new value is smaller than δ_{MPP}, which would lead the TEGs to decrease their voltage. If this happened the TEGs' thermal conductance would increase, thus greatly degrading the thermal efficiency of the system, because a high current increases the parasitic Peltier effect within the TEG [11].

III. EXPERIMENTAL RESULTS

The complete experimental system used for the experiments is shown in Fig. 5. The buck converter sits on top of a 12Ah lead-acid battery while the microcontroller board is the attached vertically on the side of the battery. Voltage and current probes connected to an oscilloscope and thermocouples connected to a data logger are used to measure the data presented in this paper. The proposed MPPT converter is tested using a real TEG system, first

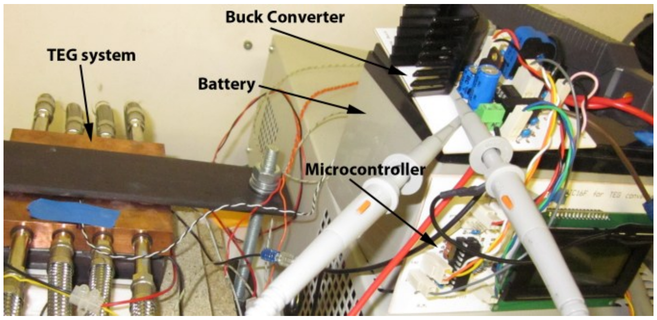

Figure 5. Picture of the experimental system used in the experiments.

characterized on its own with an electronic load in resistive mode (Fig. 2). In this way, for every operating point, at different temperature gradients, it is possible to know the maximum available power, which is the same using a resistive load or a virtual load represented by the converter. Next, the MPPT converter is connected between the TEGs and the battery load. Consequently if the MPPT converter sets the TEG voltage to $V_{OC}/2$, then the maximum available power is obtained from the TEGs, with a 100% efficiency of the MPPT algorithm. Comparing the results obtained with and without the MPPT converter at the same operating points, it is possible to understand what percentage of the maximum power that can be produced is effectively harvested by the MPPT converter.

First, the MPPT converter is tested in steady-state, with the temperature gradient across the TEGs controlled by the VEE Pro program to be 220°C. The input and output currents and voltages are presented in Fig. 6. The input power to the converter (from the TEGs) is P_{in_MPPT}=21.16W, while the maximum power harvested during the electrical characterisation is, from Fig. 2, P_{max} =21.29W. It can be concluded that the MPPT converter is very accurate, with an error of only 0.61%. The power provided to the battery is P_{out}=19.8W, which allows calculation of the electrical efficiency of the converter to be 93.6%. Fig. 6 also shows that every 100ms the input capacitors are switched out from the circuit for 467μs, during which time the microcontroller takes 8 measurements (a program cycle lasts around 60μs) of V_{OC} and then arithmetically averages the set of readings to improve precision. Within this time, the converter transfers energy from the TEGs only during t_{on} of every switching period, which accounts to less than *0.5%* of "lost" energy.

The steady-state performance of the MPPT converter shows great accuracy: it is capable of harvesting more than 99% of the maximum power available from the TEGs. Decreasing the response frequency and the number of measurements taken could slightly increase the power generated. Other than the inefficiency of energy transfer while the input capacitors are disconnected, in practice there are small quantization errors in the ADC values of V_{OC} and V_b and in the calculation of the duty cycle, but still the steady-state efficiency of the MPPT algorithm is greater than the P&O and INC methods, which are both around 95%.

Fig. 7 shows one switching period while the input capacitors are disconnected. At every t_{off} of the PWM the

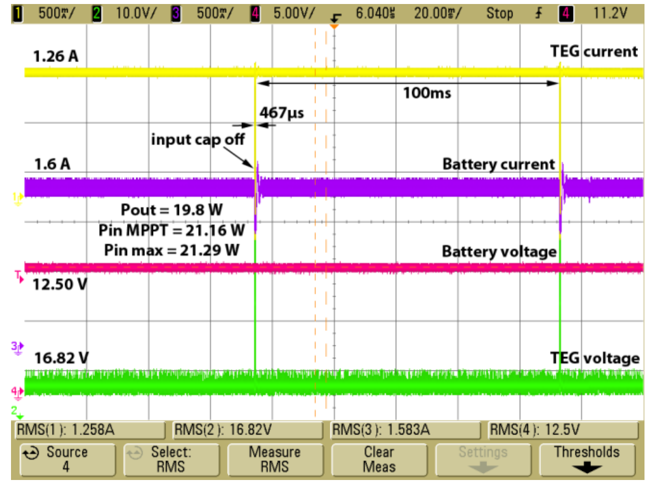

Figure 6. Steady-state performance of the MPPT converter at ΔT=220°C.

TEG current goes to zero, while the TEG voltage goes to open-circuit after a high-frequency (around 5MHz) decaying ringing of around 1μs. For this reason the ADC of the microcontroller is timed to skip the first 1μs of each t_{off} and the maximum duty cycle is set to 90%. The ringing is due exclusively to the parasitic series inductance of the TEGs and the wiring, L_σ. When the series switch suddenly opens, at the beginning of t_{off}, the current flowing in L_σ cannot reset to zero instantaneously, hence the energy contained in L_σ is dissipated in the ringing with the parasitic capacitance of the circuit. This ringing creates an over-voltage over V_{OC}, which needs to be taken into account when selecting the max drain-source voltage that the switch can stand. However, it is not dangerous for the TEGs because they can stand high levels of Joule heating and they do not contain voltage insulating layers or other materials susceptible to voltage stress.

The ability of the MPPT converter to respond to changes of the thermal input power, i.e. changes of the temperature gradient, is now assessed. In the TE generating system used, the fastest transient occurs when the electrical power to the

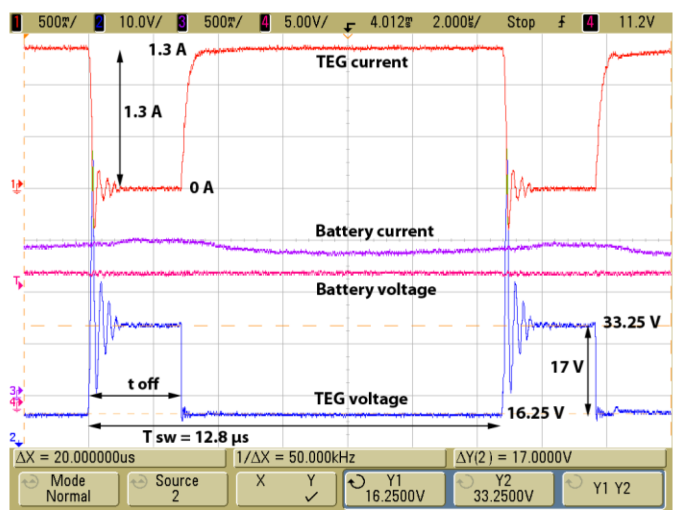

Figure 7. Switching waveforms of the TEG current and voltage when the input capacitors are switched off the circuit.

heaters is disconnected and the hot side is quickly cooled down by the water cooling system which draws thermal power through the TEGs. The test has been undertaken by setting the temperature difference to 220°C and then disconnecting the power input to the heaters. The results are presented in Fig. 8, which shows how the TEG voltage and current evolve when the system goes from the initial state of Fig. 7 down to a temperature difference of 163°C in around 2 minutes. From ΔT=170°C V_{TEG} is constant because V_{MPP} would be too close to the battery voltage, therefore the maximum allowed duty cycle has been set by the microcontroller. The dark-coloured parts of the traces are not noise, but the switching of the current to 0A and the voltage V_{OC} every 100ms (as shown in Fig. 7). Due to the way this MPPT algorithm is computed, without any integral term (like in the INC or P&O algorithms), the converter can track the MPP within 100ms, even if this time could be simply reduced by code, as explained in section II, because it was empirically determined by experience of real TE systems.

Finally the battery charging control is assessed. The following tests have been done with substitution of the battery with a power supply and a resistive load. In this way it is possible to fix the output voltage and at the same time damp the harvested current to the resistive load; the power supply will provide any excess current needed by the load. The tests were undertaken with constant input power to the heaters.

Fig. 9 shows the response of the microcontroller to changes of the battery voltage, following the routine described in section II-E. The test starts with V_b<10.2V, therefore the TEGs are set to produce the trickle current. When V_b steps to more than 10.2V the MPPT is activated. It is interesting to see how both I_{TEG} and V_{TEG} slightly decrease within the next 2.5s; this happens because during MPPT the thermal conductivity of the TEGs is higher than when the TEGs are at open-circuit, therefore the temperature gradient

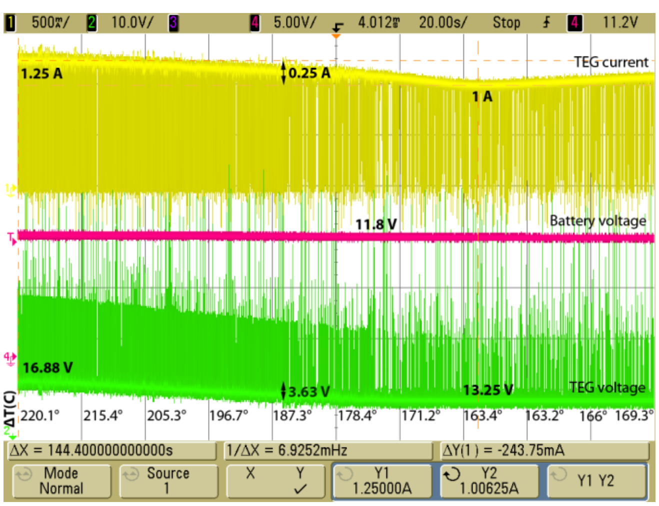

Figure 8. 140s-long transient performance of the MPPT converter from ΔT=220°C to ΔT=163°C. The emperature gradient at the beginning of every time division is written under V_{TEG}.

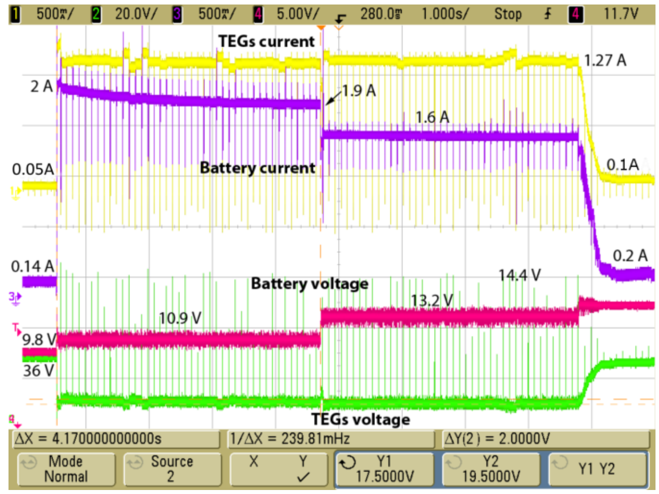

Figure 9. Response to changes of the battery voltage.

decreases. Next V_b is set to 13.2V and the microcontroller still seeks the MPP. Finally, when V_b steps to 14.4V the current drawn from the TEGs rapidly goes to I_{min}. This happens because when the microcontroller decreases the current to half of the precedent value, there is no correspondent decrease in the battery voltage, as it would happen in a lead-acid battery (Fig. 3), because the battery has been substituted with the power supply, therefore the converter continues decreasing the current until I_{min} is reached. This effect is shown in detail in Fig. 10. Immediately after the voltage step, the microcontroller sets I_{max} to 1.5A and increases the duty cycle; then it sets I_{max}=0.75A and the process goes on until I_{min} is reached. In between changes of I_{max}, the duty cycle is progressively increased at every switching period.

I. CONCLUSION

This paper presented an innovative technique to measure the open-circuit voltage of TEGs connected to a MPPT DC-DC converter, which uses the open-circuit algorithm.

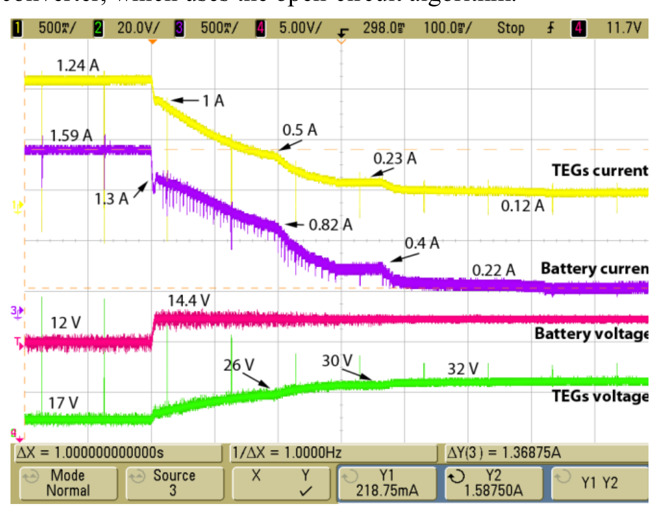

Figure 10. Reduction of the battery current after the battery voltage step.

The system is able to harvest more than the 99% of the maximum power that can be produced by thermoelectric generators and it is extremely fast and accurate, but at the same time simple and cost-effective, and can be programmed to a low-cost microcontroller. The presented system uses a 93% efficient Buck converter to store the energy harvested from real TEGs to a 12V car battery. Future work will focus on improving the performance of this method to measure the TEGs open-circuit voltage. In particular, removal of the overshoot when the TEGs are open-circuited by disconnection of the input capacitors will improve the speed of the program and reduce the number of measurement cycles required. Also, the system will be tested at higher powers and multiple converters will be interconnected to the same battery, for an application to an exhaust gas energy scavenging system.

Acknowledgment

The authors would like to thank Dr. J. Buckle of the University of Glasgow.

References

[1] B. I. Ismail and W. H. Ahmed, "Thermoelectric Power Generation Using Waste-Heat Energy as an Alternative Green Technology," *Recent Patents on Electrical Engineering*, vol. 2, no. 807, pp. 27-39, 2009.

[2] J. G. Haidar and J. I. Ghojel, "Waste heat recovery from the exhaust of low-power diesel engine using thermoelectric generators," *Proceedings ICT2001. 20 International Conference on Thermoelectrics (Cat. No.01TH8589)*, pp. 413-418, 2001.

[3] J. Yang, "Potential applications of thermoelectric waste heat recovery in the automotive industry," *ICT 2005. 24th International Conference on Thermoelectrics, 2005.*, pp. 170-174, 2005.

[4] R. Nuwayhid, A. Shihadeh, and N. Ghaddar, "Development and testing of a domestic woodstove thermoelectric generator with natural convection cooling," *Energy Conversion and Management*, vol. 46, no. 9–10, pp. 1631-1643, Jun. 2005.

[5] J. A. B. Vieira and A. M. Mota, "Thermoelectric generator using water gas heater energy for battery charging," *2009 IEEE International Conference on Control Applications*, pp. 1477-1482, Jul. 2009.

[6] T. Furue et al., "Case study on thermoelectric generation system utilizing the exhaust gas of interal-combustion power plant," *Seventeenth International Conference on Thermoelectrics. Proceedings ICT98 (Cat. No.98TH8365)*, no. 1, pp. 473-478, 1998.

[7] D. Rowe, "Thermoelectric waste heat recovery as a renewable energy source," *International Journal of Innovations in Energy Systems and Power*, vol. 1, no. 1, pp. 13-23, 2006.

[8] G. Min and D. Rowe, "'Symbiotic' application of thermoelectric conversion for fluid preheating/power generation," *Energy Conversion and Management*, vol. 43, no. 2, pp. 221-228, Jan. 2002.

[9] D. Rowe, "Thermoelectrics, an environmentally-friendly source of electrical power," *Renewable Energy*, vol. 16, pp. 1251-1256, 1999.

[10] R. Decher, *Direct Energy Conversion: fundamentals of electric power production*. Oxford University Press, 1997, p. 1997.

[11] A. Montecucco, J. R. Buckle, and A. R. Knox, "Solution to the 1-D unsteady heat conduction equation with internal Joule heat generation for thermoelectric devices," *Applied Thermal Engineering*, vol. 35, pp. 177-184, Mar. 2012.

[12] L. Chen, D. Cao, H. Yi, and F. Z. Peng, "Modeling and power conditioning for thermoelectric generation," *2008 IEEE Power Electronics Specialists Conference*, pp. 1098-1103, Jun. 2008.

[13] R.-Y. Kim and J.-S. Lai, "A Seamless Mode Transfer Maximum Power Point Tracking Controller For Thermoelectric Generator Applications," *IEEE Transactions on Power Electronics*, vol. 23, no. 5, pp. 2310-2318, 2008.

[14] I. Laird, H. Lovatt, N. Savvides, D. Lu, and V.G. Agelidis, "Comparative Study of Maximum Power Point Tracking Algorithms for Thermoelectric Generators," in *Australasian Universities Power Engineering Conference (AUPEC'08)*, 2008, pp. P-217 1-6.

[15] R.-Y. Kim, J.-S. Lai, B. York, and A. Koran, "Analysis and Design of Maximum Power Point Tracking Scheme for Thermoelectric Battery Energy Storage System," *IEEE Transactions on Industrial Electronics*, vol. 56, no. 9, pp. 3709-3716, Sep. 2009.

[16] H. Nagayoshi and T. Kajikawa, "Mismatch Power Loss Reduction on Thermoelectric Generator Systems Using Maximum Power Point Trackers," *25th International Conference on Thermoelectrics*, pp. 210-213, 2006.

[17] E. Koutroulis and K. Kalaitzakis, "Novel battery charging regulation system for photovoltaic applications," *IEE Proc.-Electr. Power Appl.*, vol. 151, no. 2, pp. 191-197, 2004.

[18] J. A. O'Connor, "Simple Switchmode Lead-Acid Battery Charger." *Unitrode U-131.*

[19] "Improved charging method for charging lead-acid batteries using the UC3906," *Unitrode U-104*, 1999.